LAXPC Calibration

H. M. Antia

antia@tifr.res.in   www.tifr.res.in/~antia

I thank all members of LAXPC and ISRO team for support and guidance.

LAXPC website: http://www.tifr.res.in/~astrosat_laxpc

- GEANT4 simulations of the detector were performed for calculating the response matrix for the detectors.
- Each simulation had 10^7 photons with fixed energy.
- Initial Photon trajectory is normal to detector top
- Uniformly distributed over detector area.
- Rejection and K-escape logic as used in processing electronics is applied in simulations also and total energy in each anode is converted to channel No.

$$n_c = e_0 + e_1 E_p (1 + e_2 E_p)$$

- The simulated spectrum is compared with observed spectrum after subtracting the background. For normalisation the simulated spectrum is multiplied by a constant to match the total counts under one peak.

- To calculate detector response for other energies we need $\sigma(E, T), n_c(E, T)$

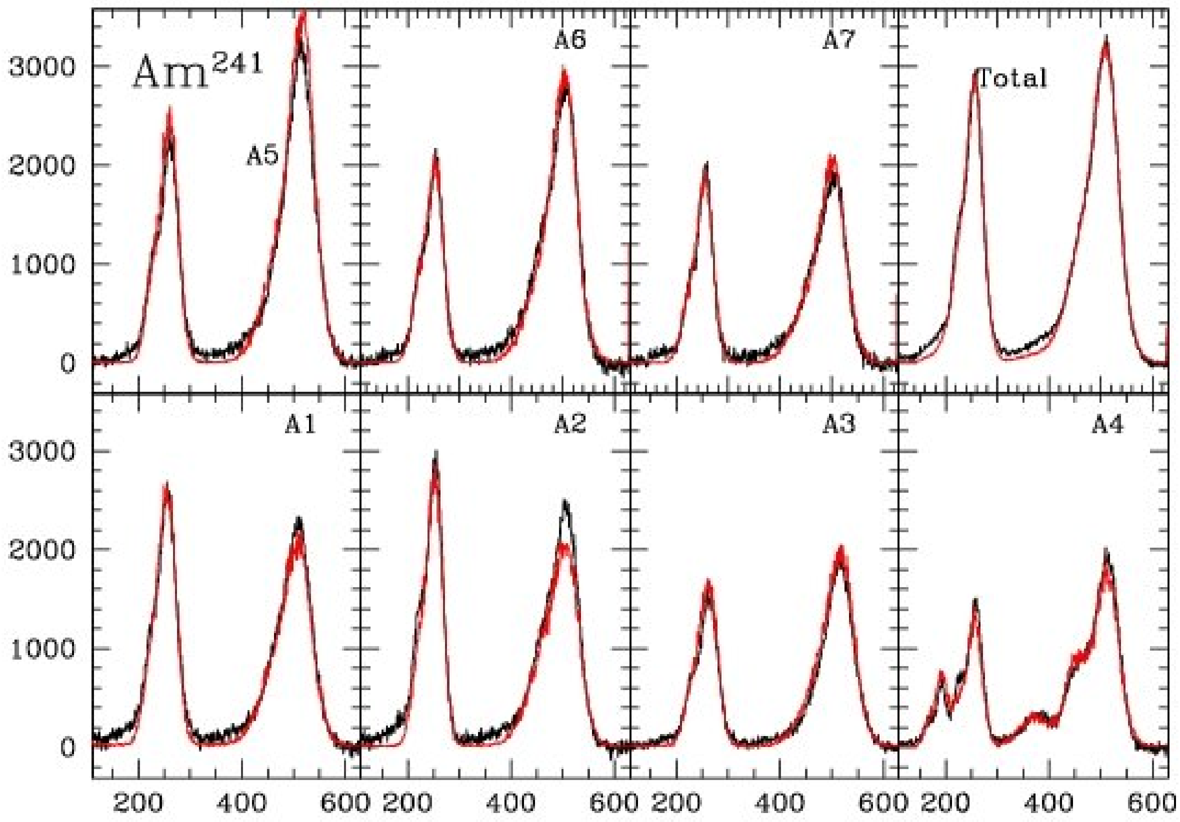

Am^{241}
A5
A6
A7
Total
A1
A2
A3
A4
3000
2000
1000
0
200
400
600

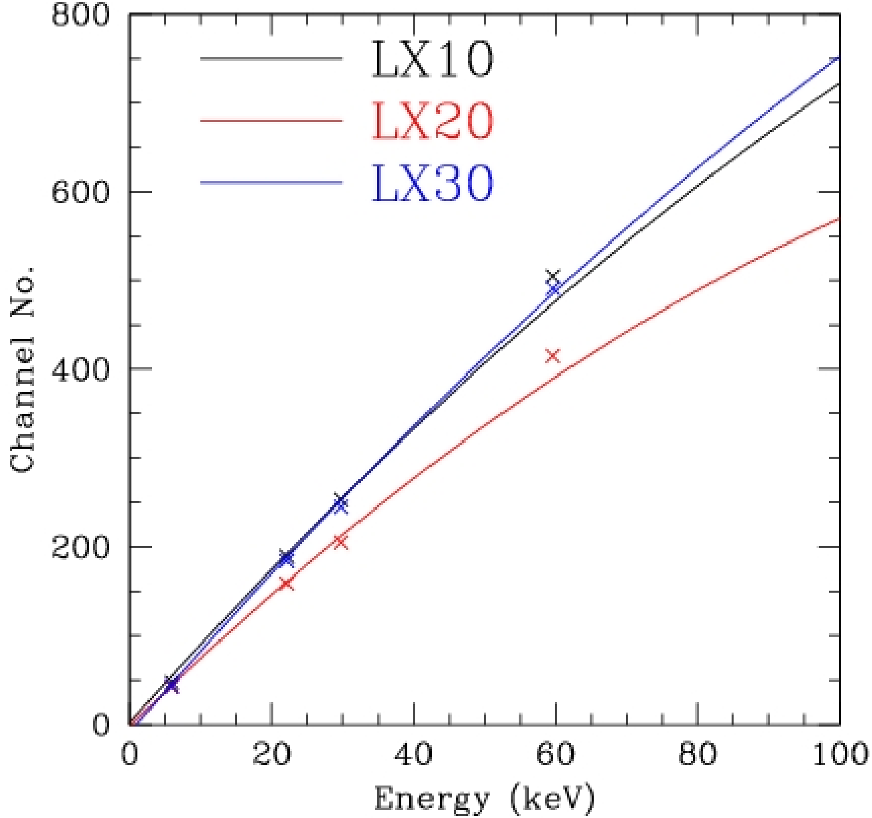

LX10
LX20
LX30
Channel No.
Energy (keV)
0
200
400
600
800
0
20
40
60
80
100

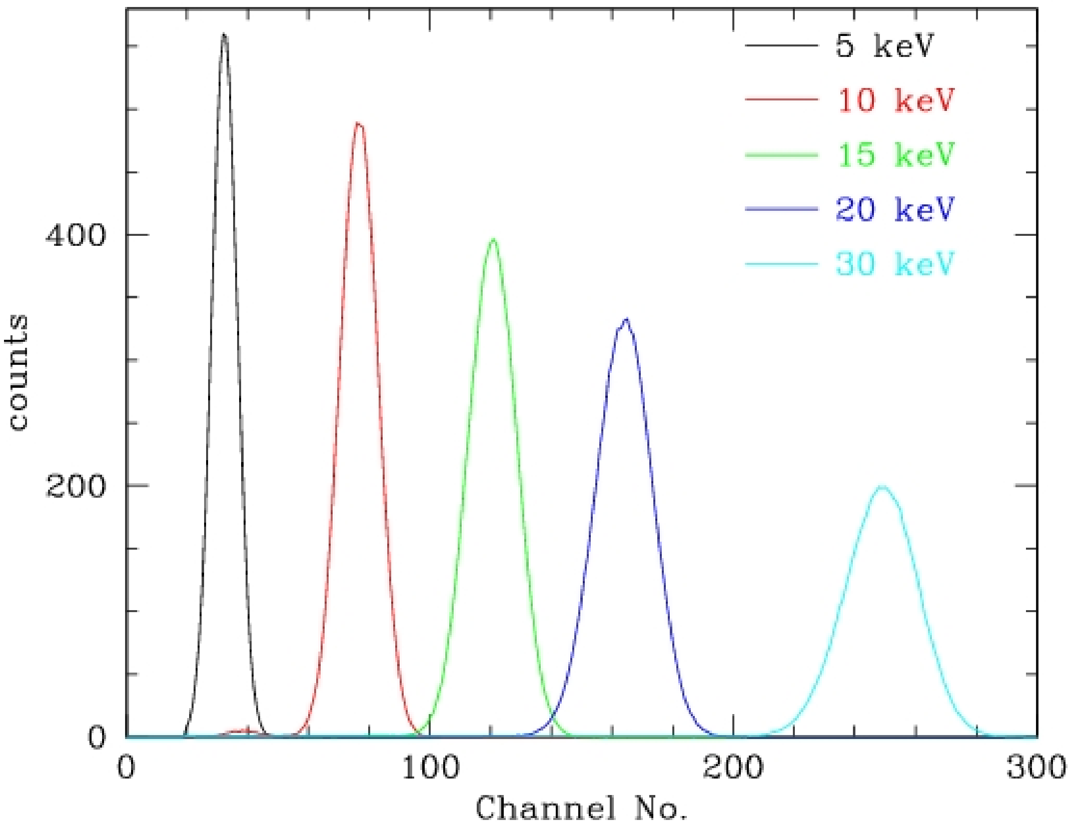
5 keV
10 keV
15 keV
20 keV
30 keV
counts
400
200
0
0
100
200
300
Channel No.

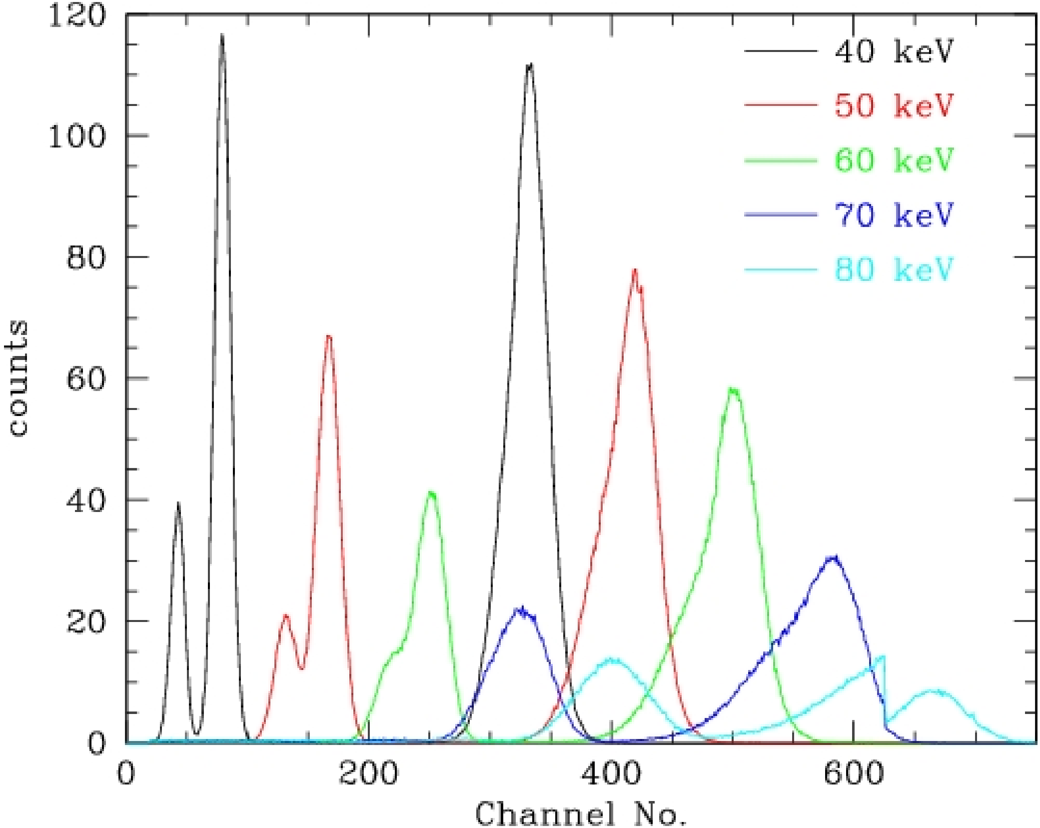

40 keV
50 keV
60 keV
70 keV
80 keV
counts
Channel No.
0
20
40
60
80
100
120
0
200
400
600

Calibration of the Field of View

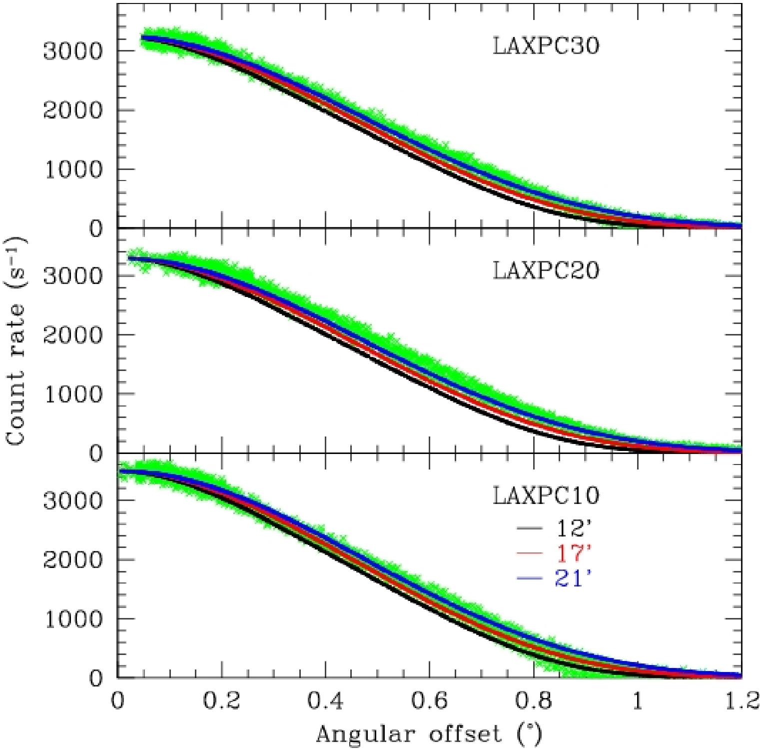

- LAXPC offset from scan on 3 February 2016

	RA ($^\circ$)	DEC ($^\circ$)	Offset ($^\circ$)
LX10	83.78	22.01	0.15
LX20	83.63	22.08	0.07
LX30	83.74	22.03	0.11
Mean	83.72	22.04	0.09
Crab	83.63	22.01	

- Satellite pointing depends on the primary payload for observations. Hence, the relative normalisation of 3 detectors should be kept free.

Detector Response Matrix

- The channel to energy mapping was adjusted to match the Crab spectrum observed after launch.
- Since the detector gain drifts with time, response matrix is generated for differing gain in the 30 keV calibration peak.
- A log of gain shift is maintained using the calibration source (Am^{241}) in veto anode A8. Normally, events recorded in anode A8 are rejected, but the detector electronics is designed to accept a small fraction of events in A8 which would include the counts due to calibration source.

- The calibration source has two peaks around 30 and 60 keV and using them it is not possible to determine the 3 coefficients in channel to energy mapping. Only the shift in 30 keV peak is used to estimate the gain shift. As a result, it is recommended to apply gain-fit while fitting the spectrum, particularly, the offset in gain, which has not been estimated. By calibrating the Crab spectrum at different times, it is possible to estimate the offset and this is provided by the software.

- To take care of even-odd fluctuation in counts with channel the no. of channels is reduced to 512 for LX10, LX30, and to 256 for LX20.
- The effect of dead-time is incorporated in the spectrum and light curve.
- To account for leak in LX30 the responses are generated with different density.
- The normalisation for effective area is estimated by cross-calibration with NuSTAR observation.
- Inclusion of flux leakage from side of the detector which gives a hump around 30 keV from Xenon K X-rays. This effect is not fully accounted for in response matrix and in some cases it may be necessary to include an additional Gaussian around 30 keV.

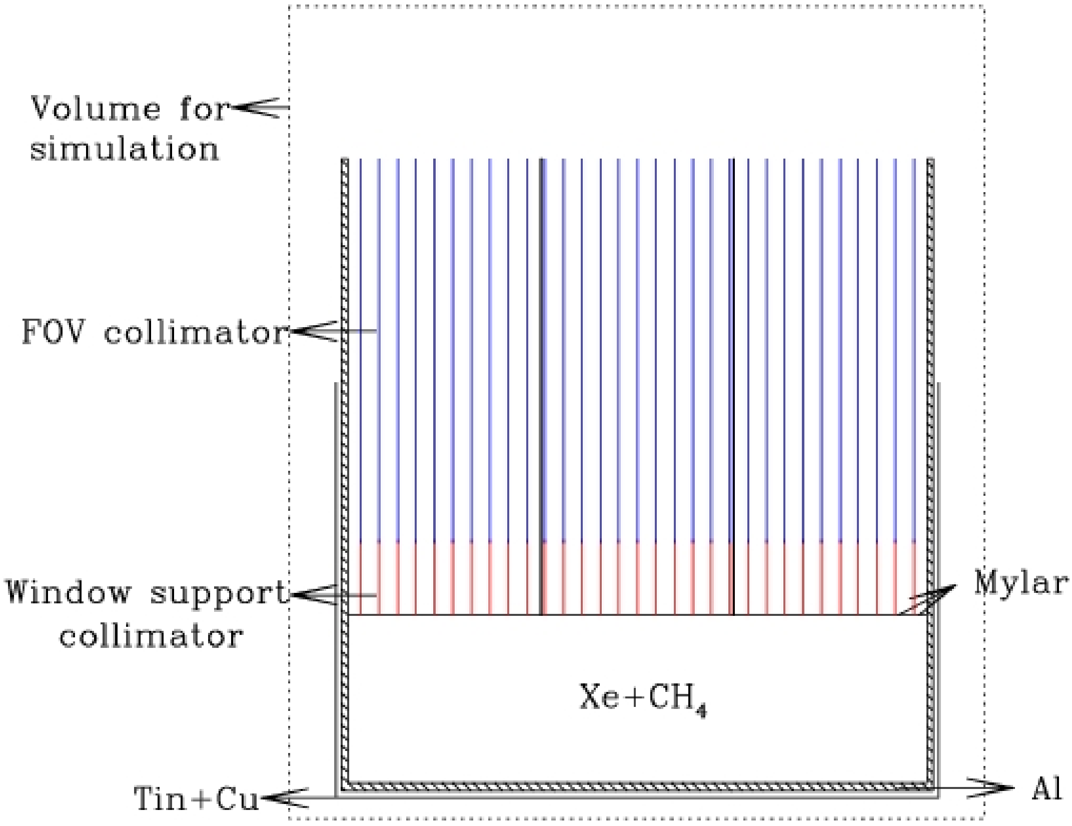
Volume for simulation
FOV collimator
Window support collimator
Mylar
Xe+CH4
Tin+Cu
Al

Fit to Crab spectrum

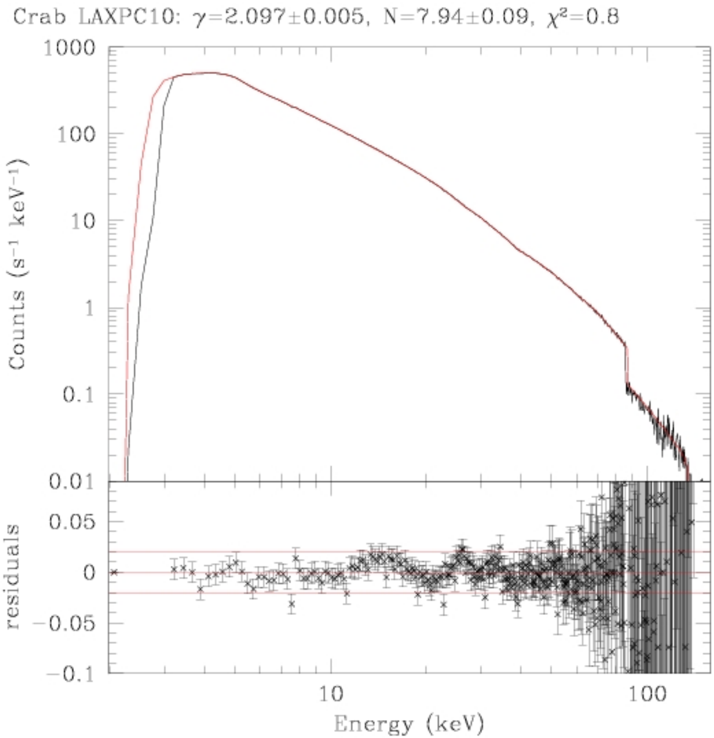

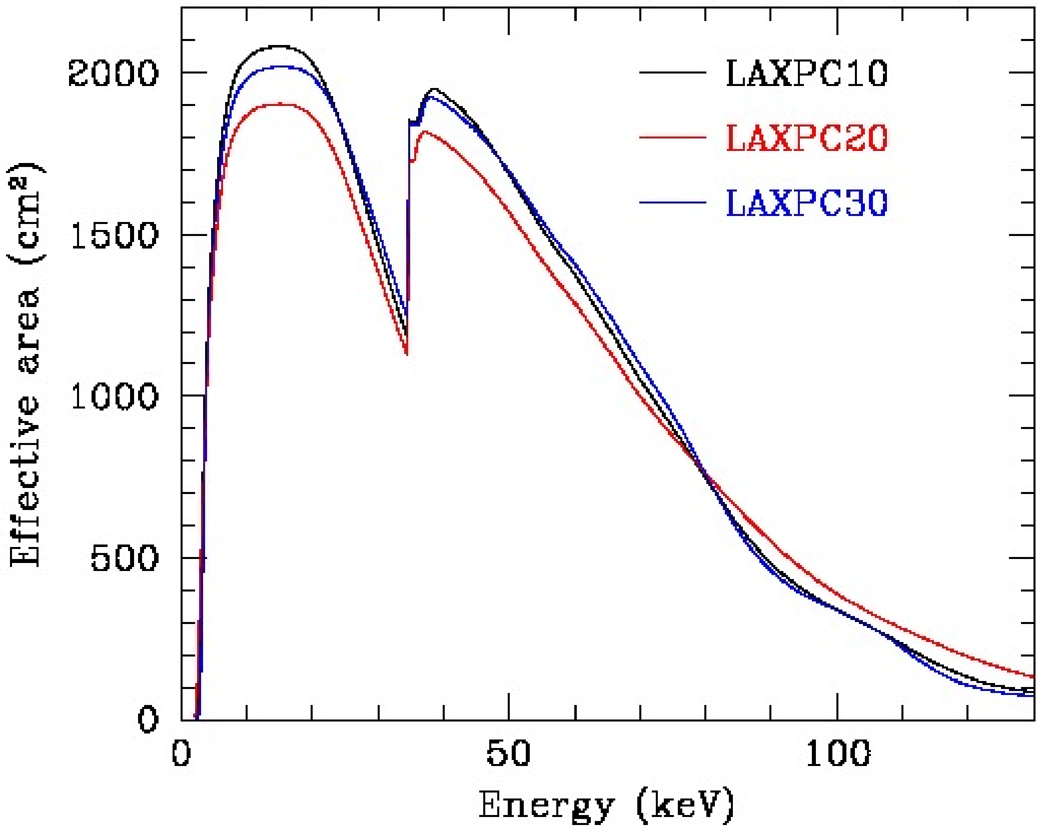

LAXPC10
LAXPC20
LAXPC30
Effective area (cm²)
Energy (keV)
0
500
1000
1500
2000
0
50
100

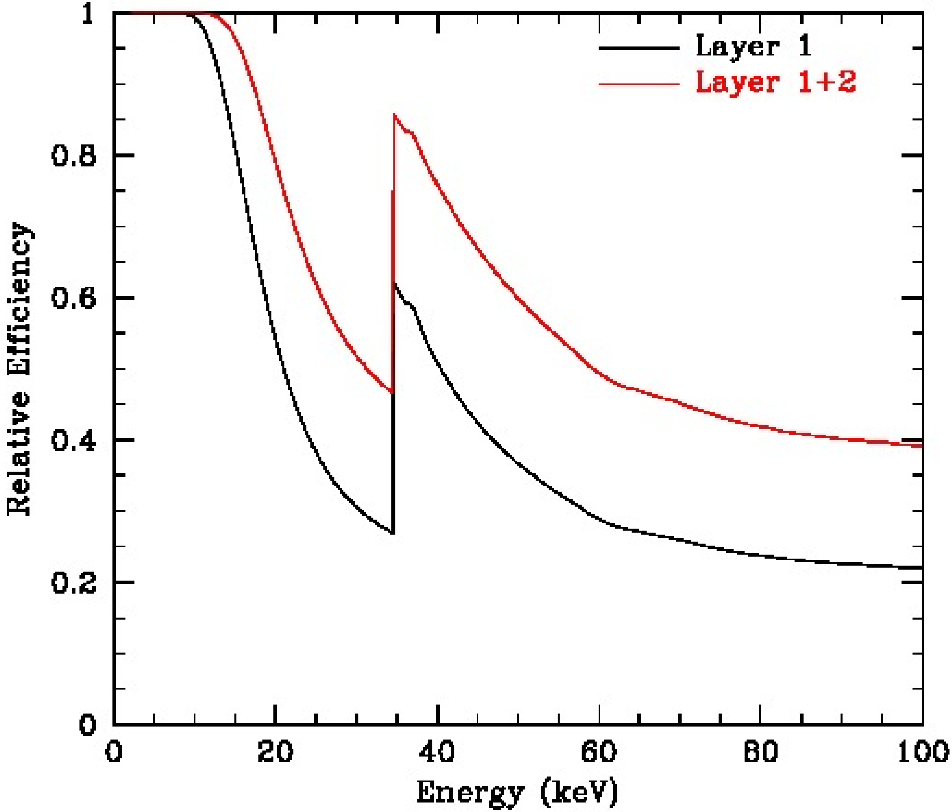
Layer 1
Layer 1+2
Relative Efficiency
Energy (keV)
0
0.2
0.4
0.6
0.8
1
0
20
40
60
80
100

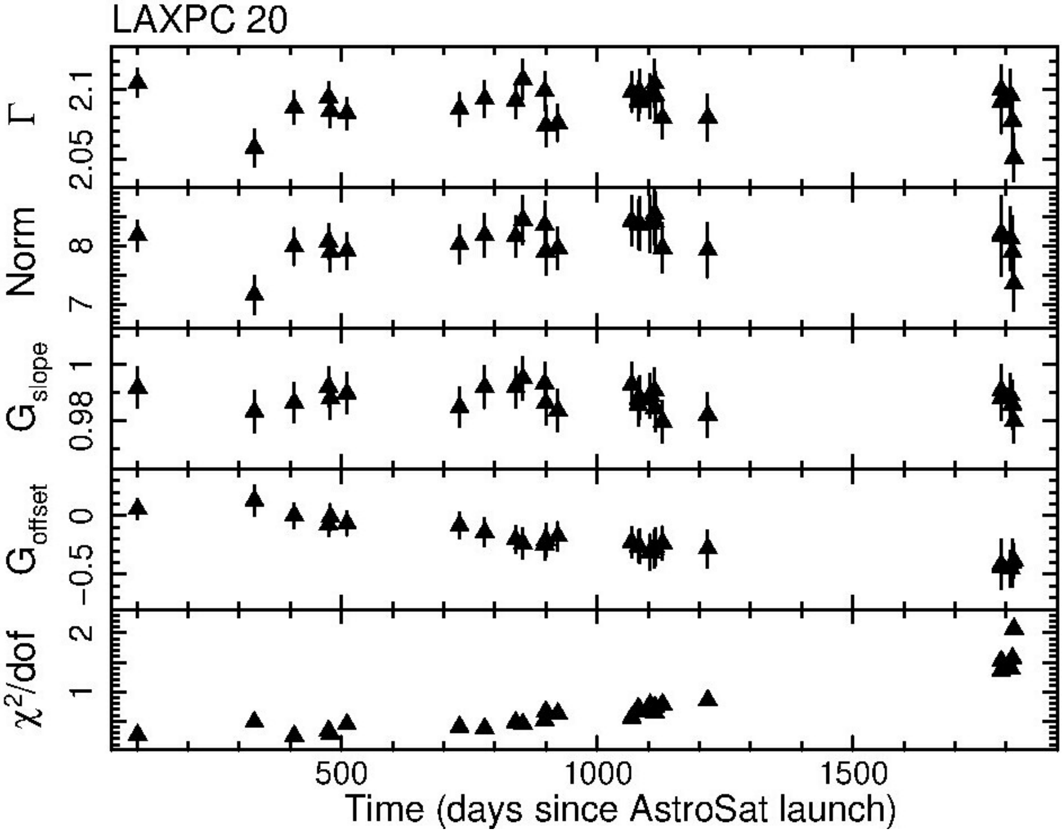

LAXPC 20
Γ
2.05
2.1
Norm
7
8
G_{slope}
0.98
1
G_{offset}
−0.5
0
χ^2/dof
1
2
500
1000
1500
Time (days since AstroSat launch)

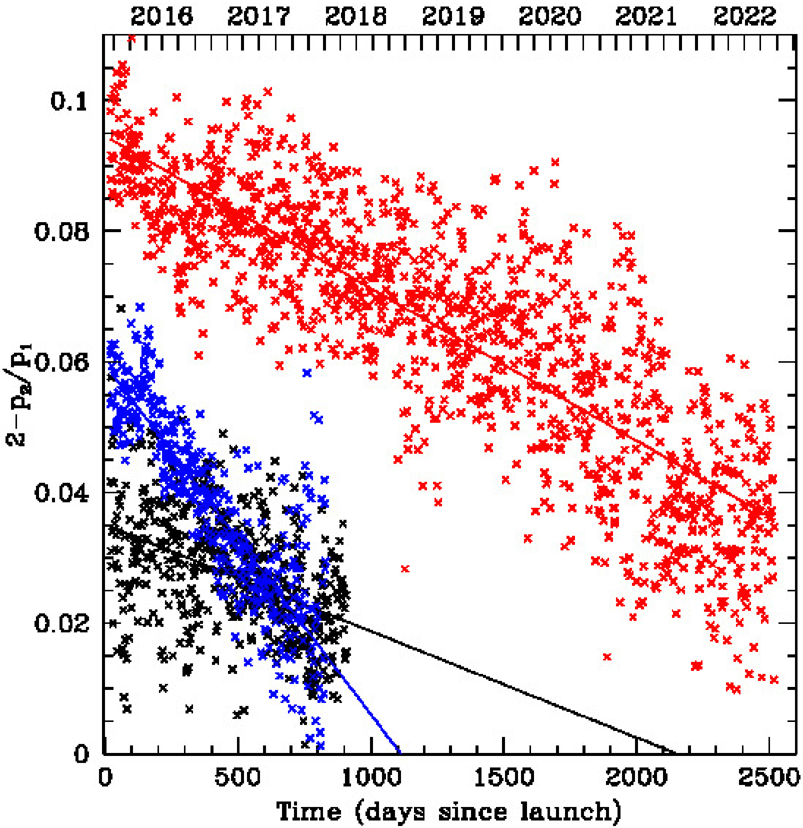

2016
2017
2018
2019
2020
2021
2022
0.1
0.08
0.06
0.04
0.02
0
$2-P_2/P_1$
0
500
1000
1500
2000
2500
Time (days since launch)

Effect of Geomagnetic Storms

8 September 2017 $(Kp = 8^{+})$

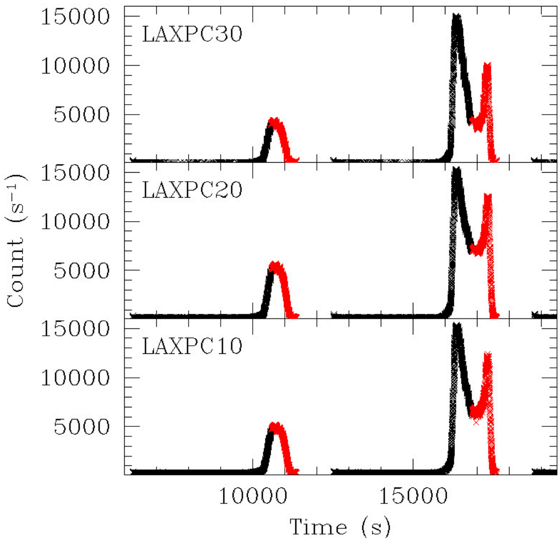

28 May 2017 $(Kp = 7)$

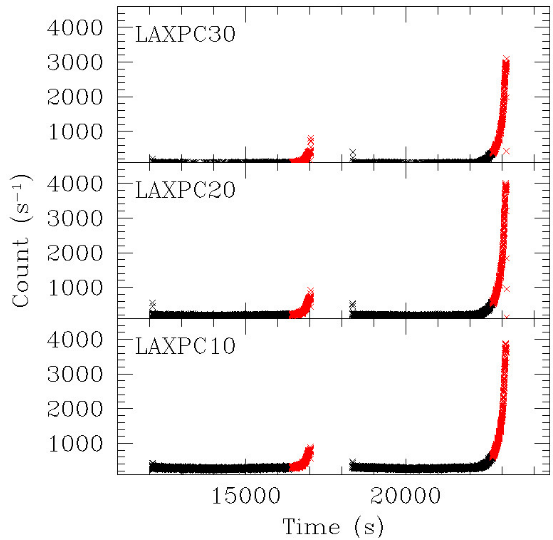

- Because of the large FOV there can be contamination from another source in the FOV. Even sources $> 60'$ can make significant contribution

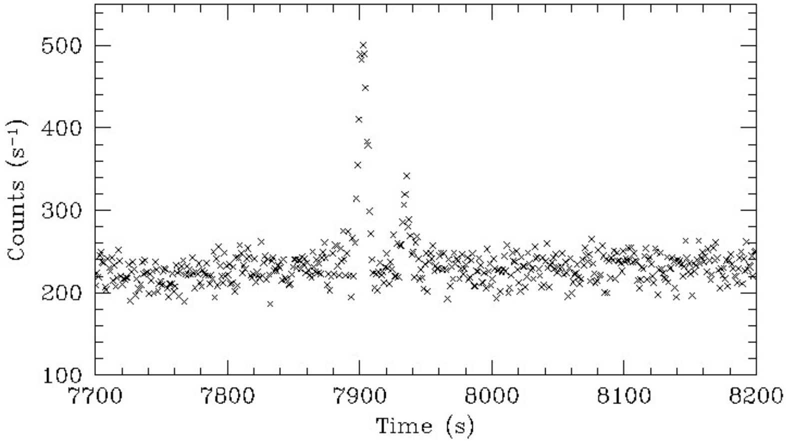

The bigger peak in this SLEW observation is due to GX 5–1 (offset $51'$, 10%) and smaller peak is due to GX 9+1 (offset $62'$, 5%)

Response with offset

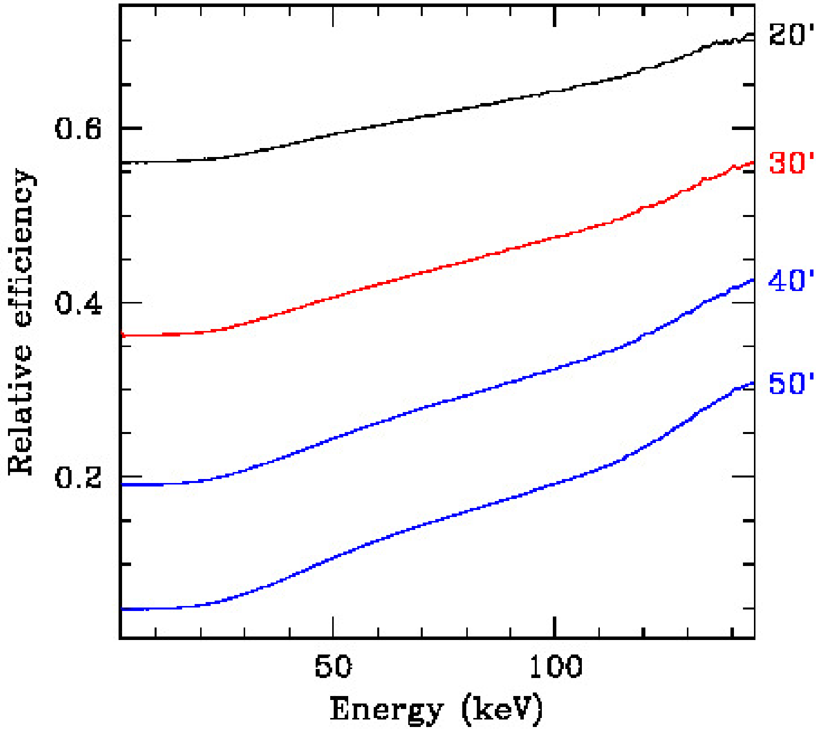

Background Model

- Different models have been tried

1. Fitting background count rate as a function of latitude and longitude (sensitive to temporal variation)

2. For faint sources, we can use counts at high energy to scale the background (R. Misra et al. 2021) (sensitive to temporal variation and gain shift)

3. Observation during Earth Occultation (affected by Earth albedo/shadow)

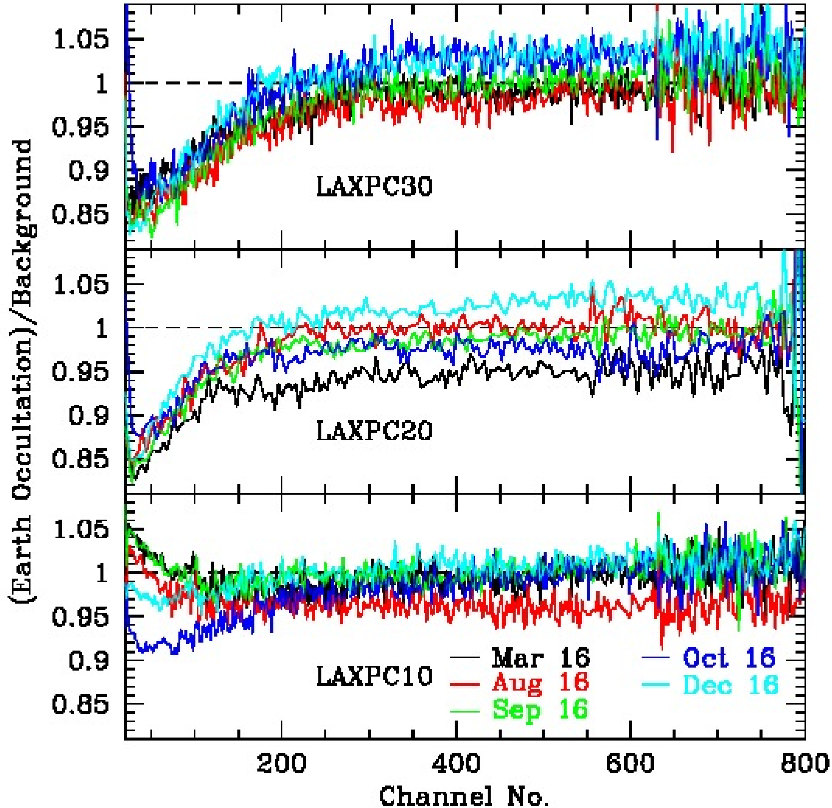

(Earth Occultation)/Background
1.05
1
0.95
0.9
0.85
LAXPC30
LAXPC20
LAXPC10
Mar 16
Aug 16
Sep 16
Oct 16
Dec 16
200
400
600
800
Channel No.

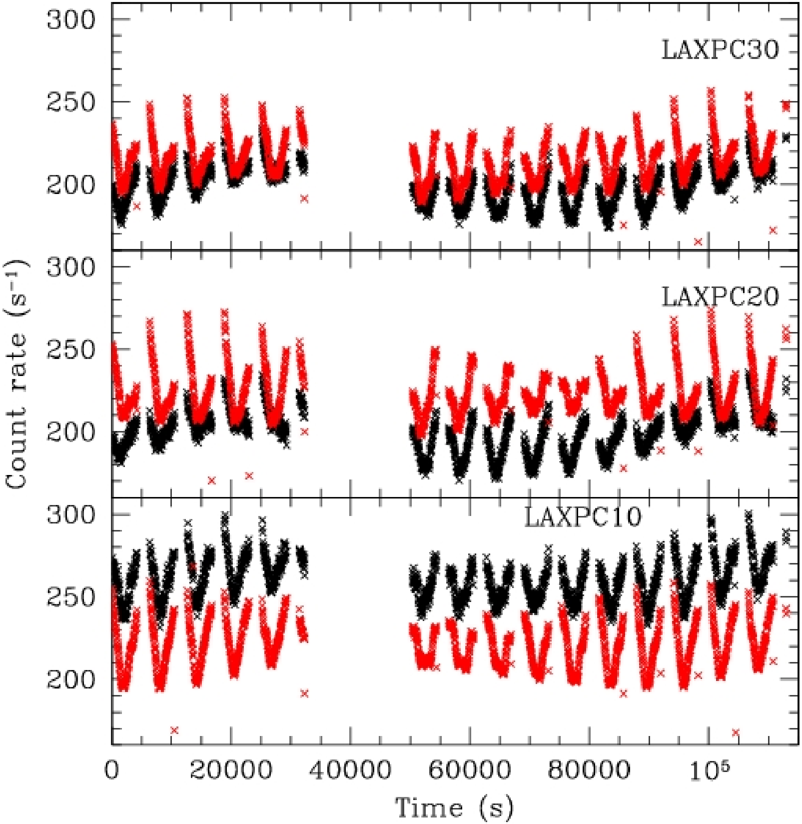

LAXPC30
LAXPC20
LAXPC10
300
250
200
Count rate (s^{-1})
0
20000
40000
60000
80000
10^5
Time (s)

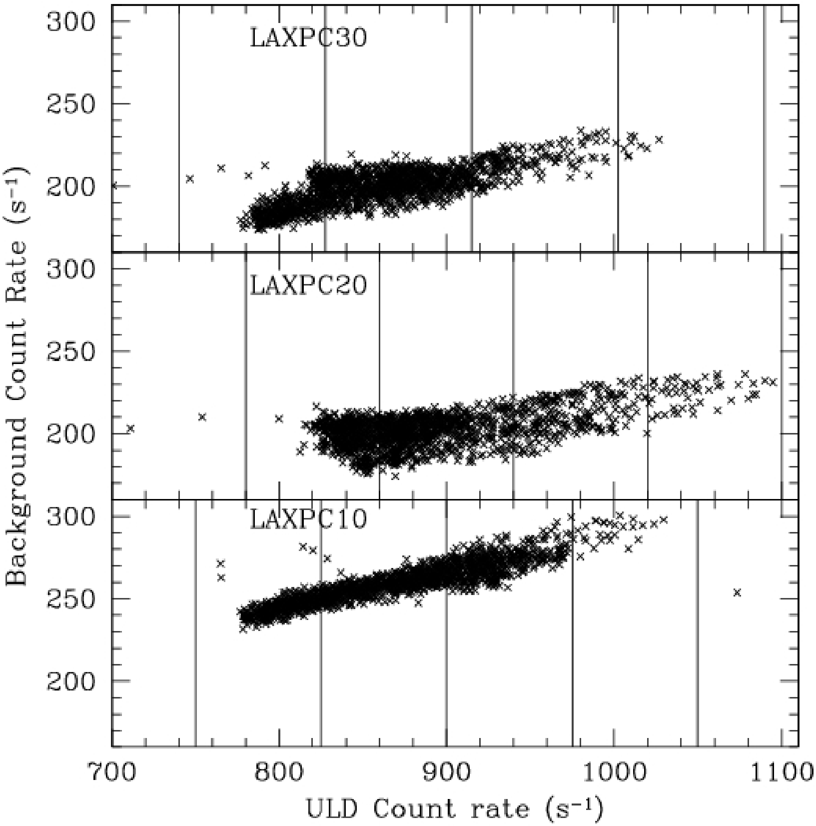

LAXPC30
LAXPC20
LAXPC10
Background Count Rate (s⁻¹)
ULD Count rate (s⁻¹)
300
250
200
700
800
900
1000
1100

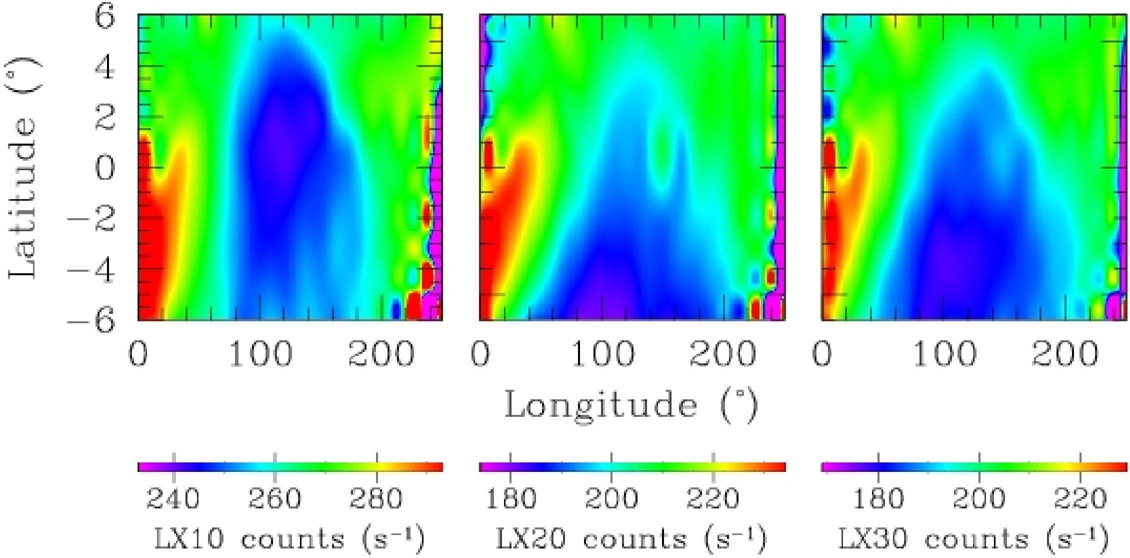

Latitude (°)
6
4
2
0
−2
−4
−6
0
100
200
Longitude (°)
240
260
280
LX10 counts (s⁻¹)
180
200
220
LX20 counts (s⁻¹)
180
200
220
LX30 counts (s⁻¹)

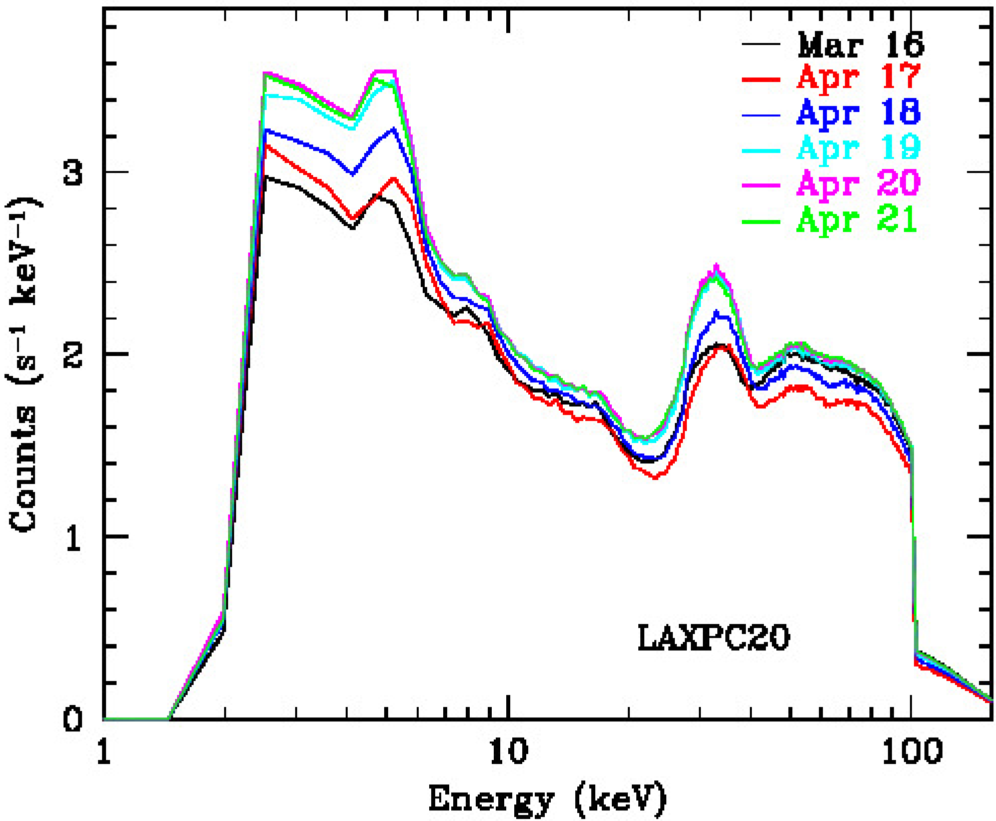

Mar 16
Apr 17
Apr 18
Apr 19
Apr 20
Apr 21
LAXPC20
Counts (s^{-1} keV^{-1})
Energy (keV)
0
1
2
3
1
10
100

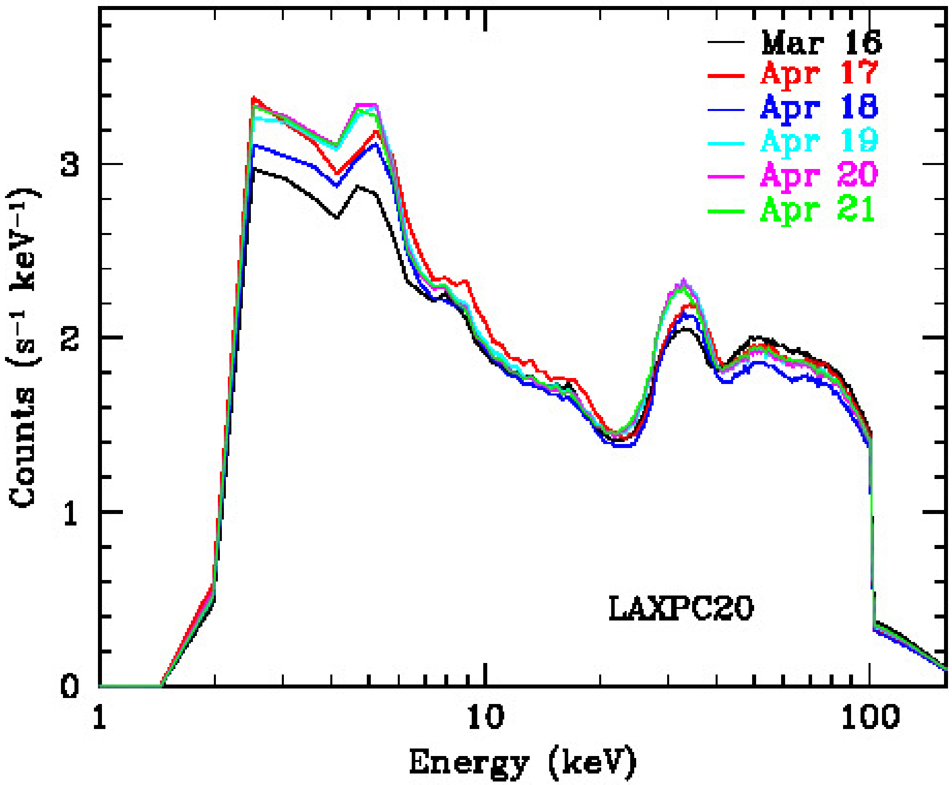

After scaling for the count rate

Updated background model

- The background counts show a quasi-diurnal variation

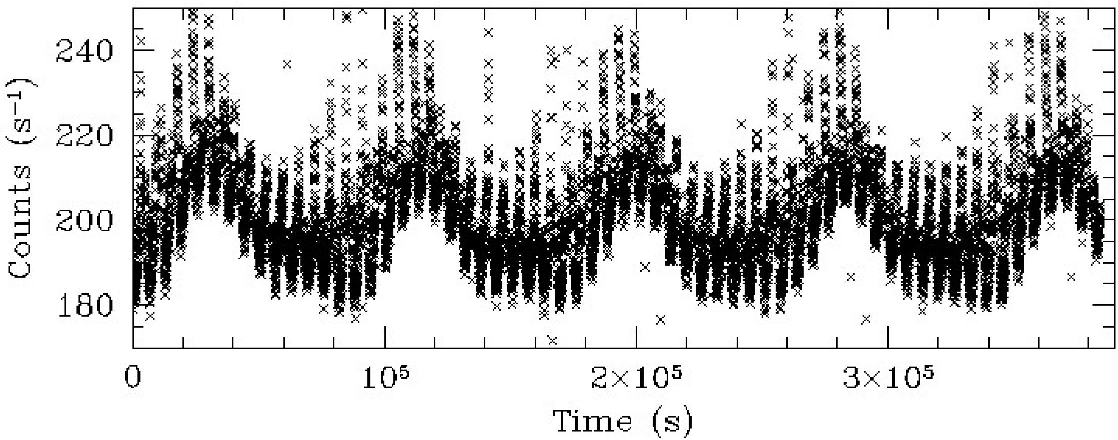

Long term variation in background counts

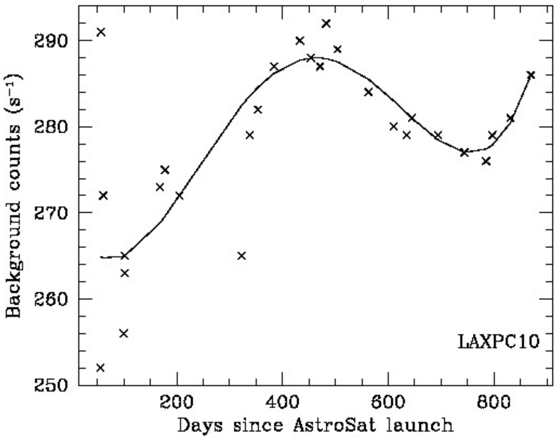

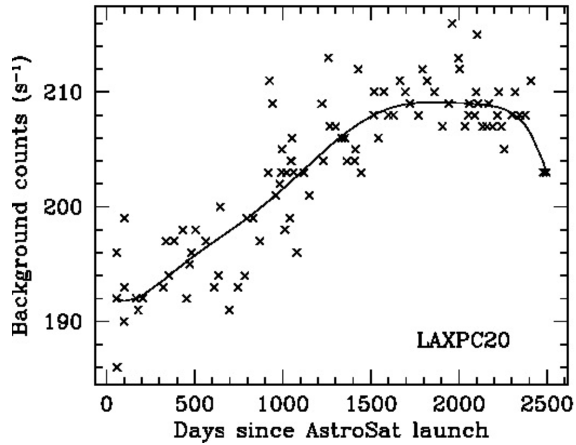

- Apart from the long term variation there is the diurnal variation which has an amplitude of about 30 s^{-1}, which is about 15% of the background counts. To remove this variation it was necessary to estimate the actual period of diurnal variation.

- Using over 5 years of background observation the period of diurnal variation was determined to be 84495 s. This appears to the diurnal period corrected for precession of the orbit.

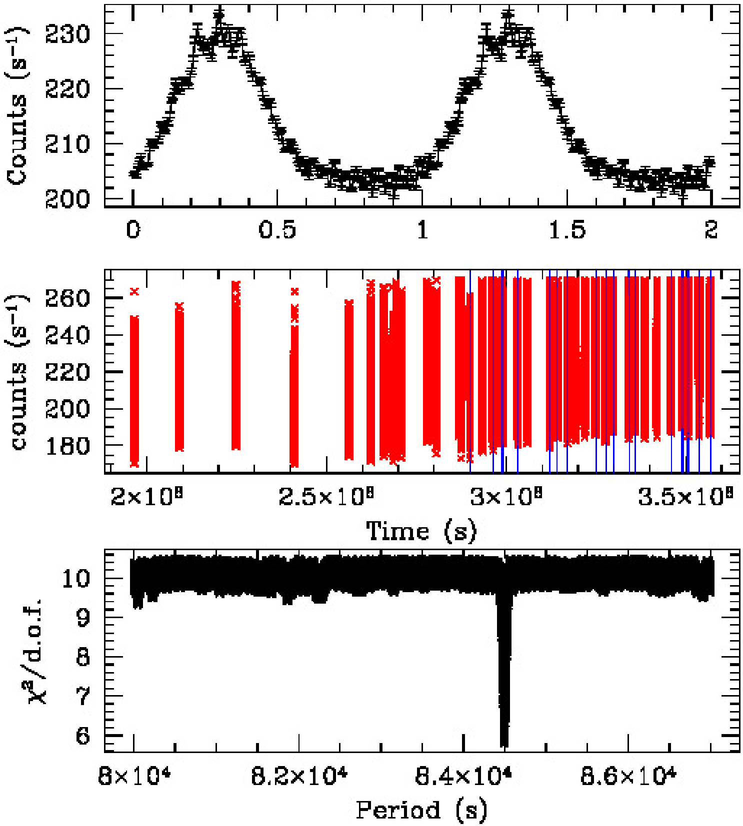
Counts (s^{-1})
230
220
210
200
0
0.5
1
1.5
2
counts (s^{-1})
260
240
220
200
180
2×10^8
2.5×10^8
3×10^8
3.5×10^8
Time (s)
χ^2/d.o.f.
10
9
8
7
6
8×10^4
8.2×10^4
8.4×10^4
8.6×10^4
Period (s)

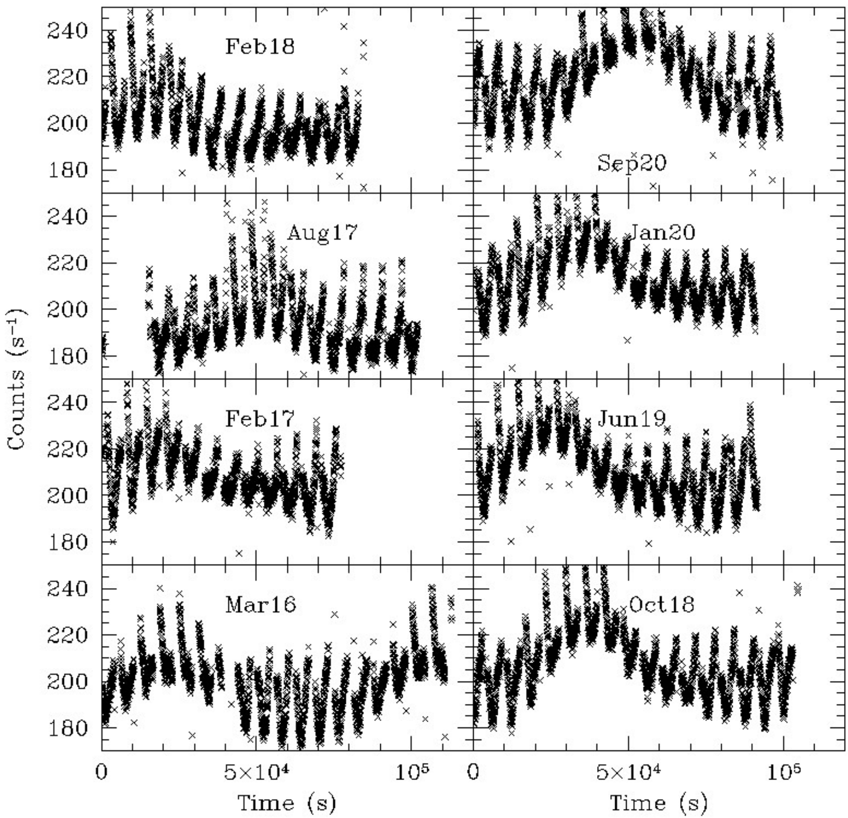
Feb18
Sep20
Aug17
Jan20
Feb17
Jun19
Mar16
Oct18
Counts (s⁻¹)
Time (s)
Time (s)
240
220
200
180
0
5×10⁴
10⁵

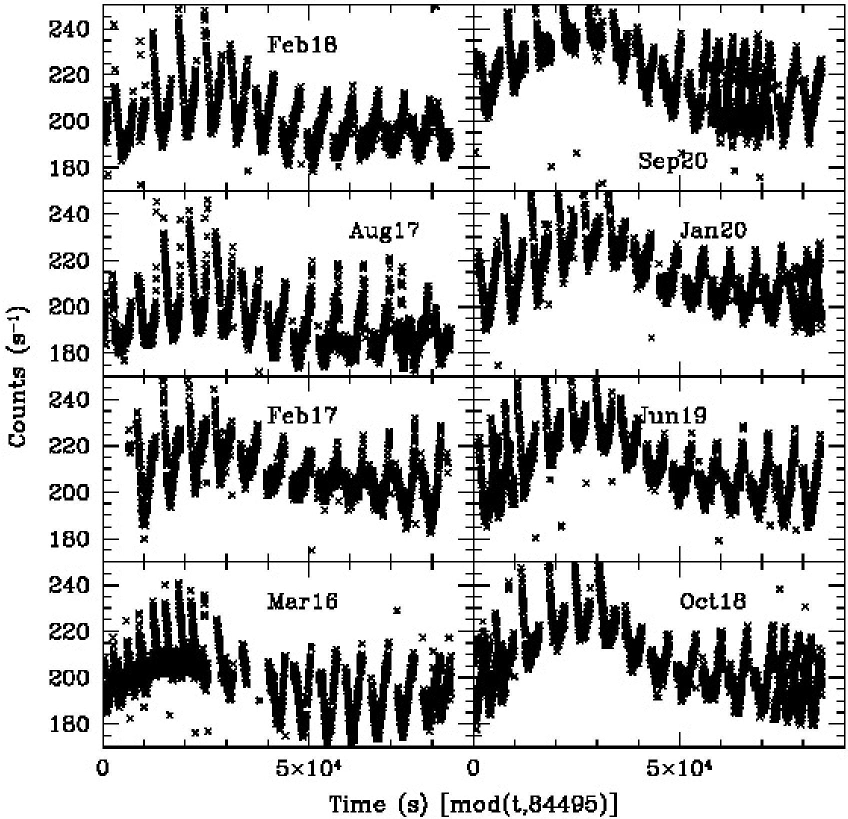
Feb18
Sep20
Aug17
Jan20
Feb17
Jun19
Mar16
Oct18
240
220
200
180
Counts (s^{-1})
0
5×10^4
Time (s) [mod(t,84495)]

Nov 2020 background

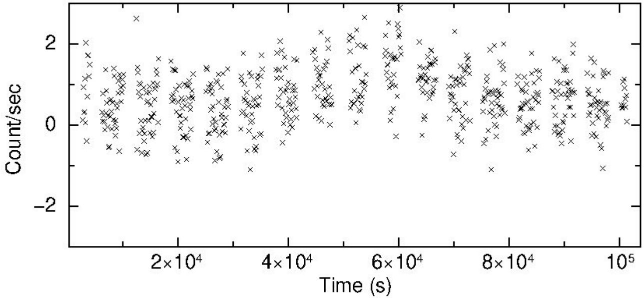

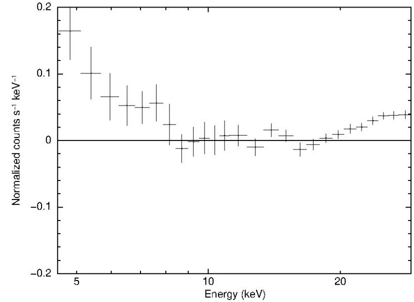

Feb 2017 background

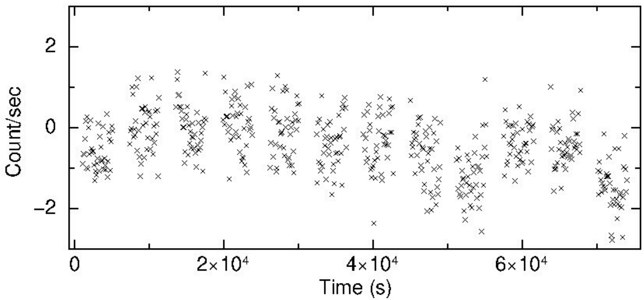

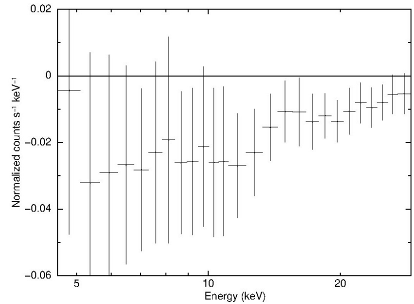

Background model for faint sources, only top layer

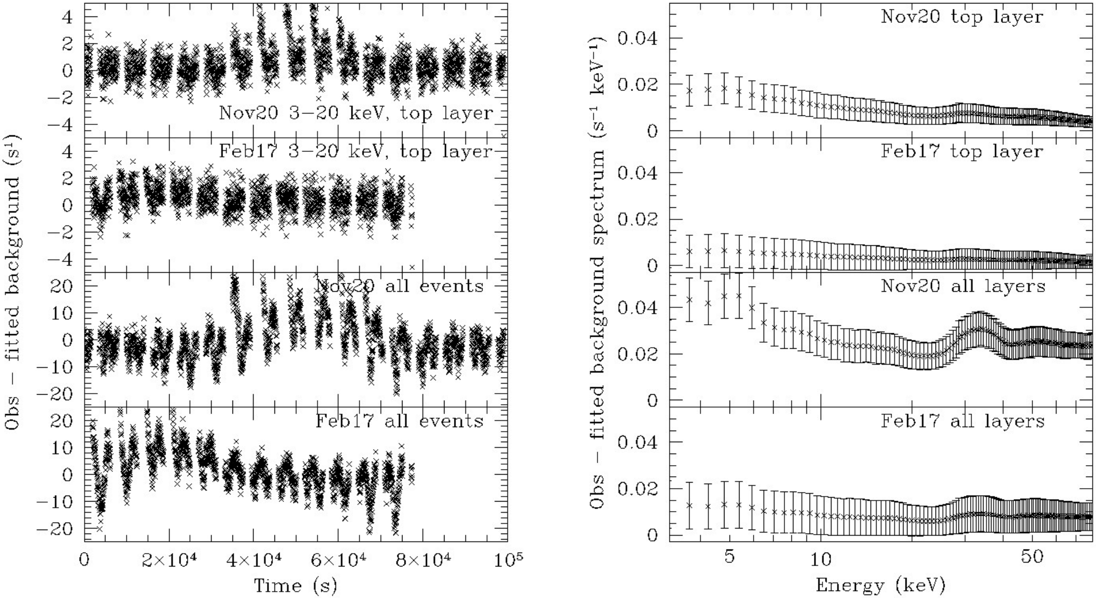

Background fit to lat and lon

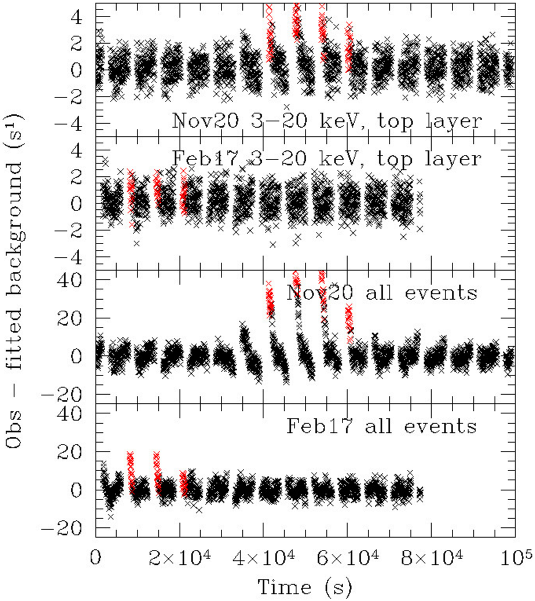

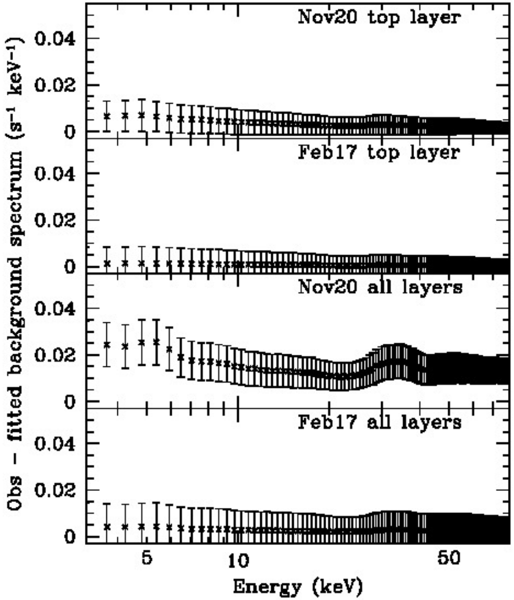

Background fit to lat and lon after correcting for diurnal variation